



HAL
open science

Sedimentary coastal cliffs of Normandy: Modalities and quantification of retreat

Stéphane Costa, Olivier Maquaire, Pauline Letortu, Guillaume Thirard, Vincent Compain, Thomas Roulland, Mohand Medjkane, Robert Davidson, Kevin Graff, Candide Lissak, et al.

► To cite this version:

Stéphane Costa, Olivier Maquaire, Pauline Letortu, Guillaume Thirard, Vincent Compain, et al.. Sedimentary coastal cliffs of Normandy: Modalities and quantification of retreat. *Journal of Coastal Research*, 2019, 88 (sp1), pp.46-60. 10.2112/SI88-005.1 . hal-02280608

HAL Id: hal-02280608

<https://normandie-univ.hal.science/hal-02280608v1>

Submitted on 15 Dec 2020

HAL is a multi-disciplinary open access archive for the deposit and dissemination of scientific research documents, whether they are published or not. The documents may come from teaching and research institutions in France or abroad, or from public or private research centers.

L'archive ouverte pluridisciplinaire **HAL**, est destinée au dépôt et à la diffusion de documents scientifiques de niveau recherche, publiés ou non, émanant des établissements d'enseignement et de recherche français ou étrangers, des laboratoires publics ou privés.

1 Sedimentary Coastal cliffs of Normandy: modalities and quantification of retreat

2 Stéphane Costa^{*a}, Olivier Maquaire^a, Pauline Letortu^b, Guillaume Thirard^a, Vincent Compain^a,
3 Thomas Roulland^a, Mohand Medjkane^a, Robert Davidson^a, Candide Lissak^a, Kevin Graff^a, Christophe
4 Delacourt^c, Timothée Duguet^d, Cyril Fauchard^e, Raphael Antoine^e.

5
6 a- Caen Normandie University, Unicaen, CNRS, LETG-Caen, 14000, Caen, France. *Corresponding
7 author : stephane.costa@unicaen.fr

8 b- University of Bretagne Occidentale, CNRS, LETG-Brest, IUEM, Rue Dumont d'Urville, 29280
9 Plouzané, France

10 c- University of Bretagne Occidentale, CNRS, LGO, IUEM, Rue Dumont d'Urville, 29280 Plouzané,
11 France

12 d – Le Havre Normandie University, CNRS LOMC, Rue Philippe Lebon, 76600 Le Havre

13 e - CEREMA Normandie-Centre, Rouen, France

14 Abstract :

16 The Normandy cliffs studied in this paper correspond to the north-western termination of the Paris
17 sedimentary basin. The latter is characterized by the existence of more or less high, undulating and
18 sometimes faulted plateaus, explaining the lithostratigraphic diversity of the outcrops, and the variety
19 of types of cliff falls and gravitational landslides encountered. These plateaus are carved into cliffs
20 with much faster retreat due to the outcropping of sedimentary formations (from the Jurassic to the
21 Upper Cretaceous) favorable to weathering. Spatial and temporal variations of Norman sedimentary
22 cliff retreat rates over multi-temporal data are examined. Data are derived from historical maps and air
23 photographs but also from recent lasergrammetric and photogrammetric monitoring. These latter
24 measures are on specific sites monitored at high frequency and resolution. The diachronic analysis of
25 all these data gives retreat rates in line with the international literature, 0.2-0.3 m/yr. The spatial
26 variations of the cliff retreat rates, at the Normandy scale, can be explained by geological structure,
27 especially at the cliff foot, but also by the influence of cliff collapses or anthropogenic obstacles that
28 disrupt the longshore drift (rates can be multiplied by 2). The contribution of the recent
29 lasergrammetric and photogrammetric techniques shows along the Norman cliffs (1) the spatial
30 distribution of the retreat or evolution rates on the cliff face. For chalk cliff of Seine Maritime, the
31 ablation rate evaluated by TLS (Terrestrial Laser Scan) on active cliffs over a period of 7 years
32 corroborates that established by photo-interpretation (observed over nearly 50 years), i.e. around 36
33 cm/year for the cap d'Ailly and almost zero for the abandoned cliffs of Dieppe; scree movements
34 (debris falls) represent 100% of the evolution of the abandoned cliff faces while they account for 2%
35 of the total retreat of the active cliff of cap d'Ailly. About the rhythms, multi-temporal data shows that
36 the temporalities evolution of cliff extends from 1 to 7 decades according to the lithology. The high
37 resolution and frequency monitoring provide also some information about the factors responsible for
38 triggering gravitational landslides (rockfall, slide, debris fall). For the cliff characterized by landslides
39 (Villerville et Vaches Noires), which are under the dominating influence of the rainfall and the
40 groundwater level evolution, the study proposed a regional warning, especially in cases in which the
41 piezometer of the site exceed a depth of 11m (Groundwater Level) and the effective rain on a 4-
42 months-period is over 250 mm. In this respect, and for chalk and limestone cliffs, the monitoring is
43 inconclusive, because the origin of evolutions is more multifactorial.

44 Introduction:

45 Before the 1990s, the vast majority of coastal geomorphology work focused on accumulation coasts,
46 due to the presence of many economic challenges threatened by rapid regressive changes, or
47 potentially accelerated by contemporary mean sea level rise (Trenhaile, 2000; Woodroffe, 2002;
48 Kennedy *et al.*, 2017). However, rocky and cliffy coasts are said to represent more than 75% of the
49 world's coastline (Emery and Kuhn, 1982; Davis and Fitzgerald, 2003), and are now one of the few
50 sources of sediment for beaches. It is only in the last two to three decades that studies on these
51 retreating coasts have increased (Kennedy *et al.*, 2014; Kennedy *et al.*, 2017). This is probably due to
52 the rising impact of their retreat on coastal activities and populations, and to the development of tools

53 and methods to understand the slow but abrupt dynamics of these complex rocky coastal systems
54 (Sunamura, 1992; Paskoff, 1998; Bird, 2000; Brunnsden and Lee, 2004; Young *et al.*, 2009; Costa *et al.*,
55 *et al.*, 2004; Costa *et al.*, 2004; Gomez-Puyol *et al.*, 2014; Letortu *et al.*, 2015b; Guiliano, 2015). The
56 Norman morphostructural environment (between the Bay of Mont Saint Michel and the Tréport) is
57 favorable to the development of retreating coasts, the evolution of which can be very important
58 (Maquaire, 1990; Costa, 1997; Costa *et al.*, 2004; Lissak, 2012; Elineau, 2013; Lissak *et al.*, 2013;
59 Letortu *et al.*, 2015b; Maquaire *et al.*, 2013; Medjkane *et al.*, 2018). To the extreme west of the study
60 area (Cotentin) appears the Armorican Massif (Fig. 1) composed of ancient sedimentary, metamorphic
61 and volcanic soils (crossed locally by granitic intrusions). Rocky coasts are made up with these
62 Paleozoic materials (Dugué *et al.*, 1998) with very slow retreat. In the rest of the study area, to the
63 north, the ancient Armorican lands are covered, sometimes in discordance, by the northwestern
64 termination of the Paris sedimentary basin (Juignet, 1974; Lasseur, 2007; Le Cossec, 2010;
65 Benabdellouahed *et al.*, 2014). The latter is characterized by the existence of more or less high,
66 undulating and sometimes faulted plateaus, explaining the lithostratigraphic diversity of the outcrops,
67 and the variety of types of gravitational landslides encountered. Thus, in contact with the
68 epicontinental sea that is the Eastern and Central Channel, these plateaus are carved into cliffs with a
69 much faster retreat due to the outcropping of sedimentary formations (from the Jurassic to the Upper
70 Cretaceous) favorable to weathering. This article has a twofold objective: first, to provide, on a
71 historical scale and using traditional photo-interpretation methods, the values of the retreat of Norman
72 sedimentary cliffs. In a second step, and on specific sites monitored at high frequency and resolution
73 (SNO-Dynalit and SNO-OMIV sites, photogrammetric and lasergrammetric monitoring), the objective
74 is to provide initial results on some of the main issues that drive the research community working on
75 cliff coasts, namely, the spatial distribution of the retreat or evolution rates on the cliff face, the
76 evolution rhythms, and the factors responsible for triggering gravitational landslides (rockfall, slide,
77 debris fall).

78

79 **1/ Study area**

80 The coastal cliffs studied in this paper exclude cliffs carved from Paleozoic rocks in the Cotentin
81 region (from Saint Vaast la Hougue to Bay of Veys). The Norman cliffs studied therefore correspond
82 to the north-western termination of the Paris sedimentary basin and have an average amplitude of
83 about fifty meters, even if they can exceed 100 m in the Seine Maritime area. At the foot of the latter is
84 a large shore platform (150 to 700 m wide), with a low slope (0.2 to 2%), sometimes covered with thin
85 sandy veneers. In their upper part, the shore platforms are hidden by a flint gravel barrier in Seine-
86 Maritime or resistant limestones and sands of multi-metric thickness in Calvados (Costa *et al.*, 2006).
87 With regard to the morphostructural characteristics of the study area, we can observe (Fig. 1):

88 1- To the west of Calvados, between Grandcamp-Maisy and Saint-Côme de Fresné, lie the active cliffs
89 of the Bessin plateau, which range in height from 10 to 75 m (section C-D, Fig. 1). These cliffs are
90 composite in their topographical aspects and geological structures. The profiles are variable from one
91 end to the other and in relation to the relative thicknesses between the limestones (Bajocian and
92 Bathonian stages) and the marls of Port-en-Bessin (Bathonian stage). Three types of cliffs have been
93 defined (Maquaire, 1990): a cliff with a soft marly pedestal topped by a limestone cornice, a cliff with
94 a resistant pedestal in the marly limestone of the Lower Bathonian or the limestone of the Bajocian,
95 and a simple subvertical cliff reinforced by the Bathonian limestone.

96 2- In the 'Caen Countryside', the similar system is reproduced between Saint-Aubin-sur-Mer and Lion-
97 sur-Mer with a plateau at lower altitudes. Several small areas of low active cliffs (Bathonian
98 limestone) do not exceed 10 m in height.

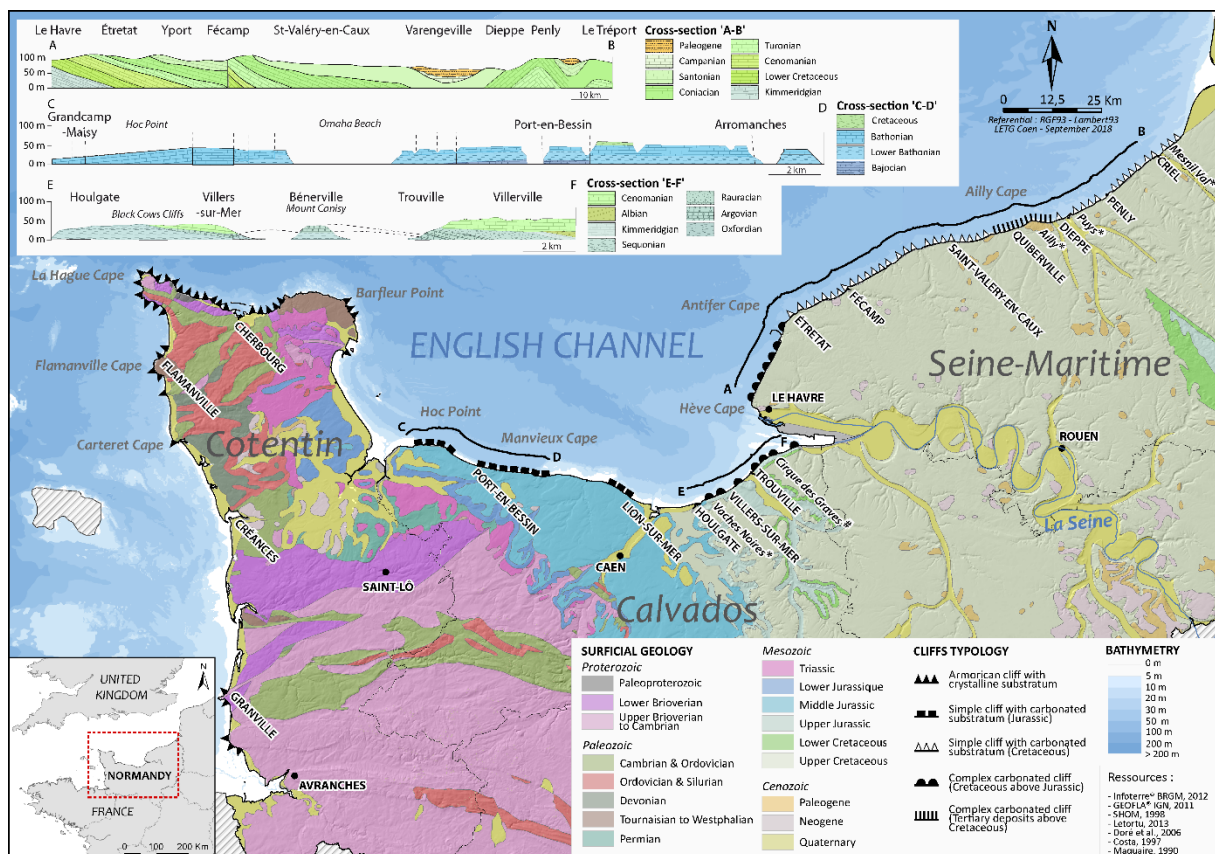
99 3- Along the plateau of the 'Pays d'Auge', the cliffs carved into the Jurassic and the Lower and Upper
100 Cretaceous are discontinuous and looser (section E-F, fig. 1). The cliffs of the 'Vaches Noires', carved
101 into the Oxfordian stage where some limestone beds are interstratified, are called mudflow cliffs,
102 forming a landscape of badlands and pinnacles. In Benerville-sur-Mer, at the right of Mont Canisy
103 (110 m), and especially between Trouville-sur-Mer and Honfleur, the cliffs reappear (section E-F, fig.
104 1). Their foot is made of Jurassic age materials (limestone and marl) topped with Albian sand (Lower

105 Cretaceous) and Cenomanian chalk (Upper Cretaceous) suitable for deep-seated landslides (Maquaire,
 106 1990; Lissak, 2012).

107 4- From Cap d'Antifer to Tréport, the cliffs are carved mainly into Upper Cretaceous chalk (from
 108 Cenomanian to Campanian stages) whose facies are more or less rich in flint beds (section A-B, fig.
 109 1). The local tectonic deformations of the Caux plateaus also explain the outcropping of some lower
 110 Jurassic and Cretaceous strata (between Octeville-sur-Mer and Le Havre), or the conservation of sandy
 111 and clay terrains of Tertiary age (Cap d'Ailly; Bignot, 1962). The different chalk layers (Pomerol *et*
 112 *al.*, 1987; Mortimore *et al.*, 2004; Lasseur, 2007) show subtle variations in resistance, also found in the
 113 cliff profile (Fig. 1). Thus, between Cap d'Antifer and Le Tréport, three types of cliffs have been
 114 defined (Costa, 1997): simple vertical cliffs (main type) composed mainly of Coniacien-Santonian
 115 chalk; cliffs with resistant pedestal, with a "basal" jump corresponding to the outcrop of the Turonian
 116 stage or even the more resistant Cenomanian stage; and complex cliffs. For the latter, the Coniacien
 117 and Santonian chalk (~ 30 m) are topped by clayey and sandy loose formations (~ 40 m), forming
 118 three back cliffs (Cap d'Ailly).

119 Variations in resistance between the various outcrops (Juignet, 1974; Dugué, 1989; Juignet and
 120 Breton, 1992; Laignel, 1997; Dugué *et al.*, 1998; Lasseur, 2007), visible in cliff profiles, reflect
 121 various gravitational mechanisms (falls, slide, flow, etc.), but also different retreat rates and evolution
 122 rhythms. The difficulty in quantifying cliff retreat lies in the slowness of the dynamics (a time taken to
 123 prepare the rock material, often several decades before the rupture), the multiplicity and sometimes the
 124 combination of marine and sub-aerial factors responsible for the dynamics, and the punctual
 125 dimension of the evolution (spatially localized phenomenon).

126



127
 128 Figure 1: Simplified geological map of the Normandy (from BRGM, French geological survey) and
 129 litho-stratigraphic profiles of cliffs on the study site.

130 Normandy is located in the northwestern part of France, on both sides of the 50th northern parallel,
 131 along the English Channel (epicontinental sea, 86 m deep on average). The environment is macrotidal

132 (Table 1) with a tidal range of 8 m (south) to 10 m (north). Waves (Table 2), which impact the cliff
 133 foot during high tide, are limited but the wind sea can produce significant wave heights of up to 4 m at
 134 Dieppe (annual return period).

Location	Barfleur	Le Havre	Dieppe	Le Tréport
Higher Astronomic Tide (HAT) (IGN69)	3.62 m	4.18 m	5.66 m	5.78
Lower Astronomic Tide (LAT) (IGN69)	- 2.98 m	- 4.08 m	- 4.52 m	- 4.43 m
Higher level observed during storm (IGN69)	4.02 m	/	5.95 m	/

135 Table 1: Tide level along the Normandy coast (Shom, 2007).

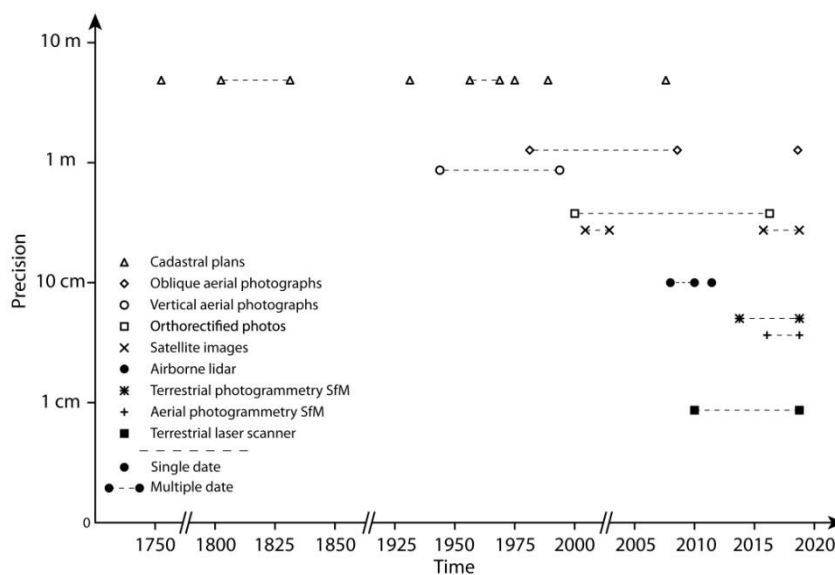
Location	Cherbourg	Le Havre	Antifer	Dieppe	Penly
Annual height	4.20 m	3.5 m	4.1 m	4.3 m	3.8 m
Decennial height	5.70 m	4.6 m	5.7 m	5.7 m	4.7 m

136 Table 2: Significant wave ($H^{1/3}$) along the Normandy coast (in Augris *et al.*, 2004; Cerema, in press).

137 Normandy has a marine west coast climate. According to data from Météo-France (1971-2000),
 138 average winter temperatures are positive but an average of 26 daily freeze/thaw cycles is recorded per
 139 year (minimal temperature can reach -15°C). Rainfall is distributed over the year (≈ 800 mm) although
 140 fall and winter are the wettest seasons (51 mm in August and 94 mm in November). Daily rainfall can
 141 exceed 77 mm in October.

142 2/ Methodology, material and documents

143 With regard to the objectives of this paper, the diachronic approach is central. Indeed, two main
 144 techniques and documents are used (Fig. 2).



145
 146 Figure 2: Techniques and documents used to study the evolution of Norman sedimentary coastal cliffs

147 2.1/ Quantification on historical scale and for all Norman sedimentary cliffs

148 This quantification (several decades) was carried out by classical photo-interpretation, then for the
 149 Calvados, by comparison with ancient cartographic documents (cadastral register and "Terrier plan" of
 150 the 19th century). The main documents used are vertical aerial photographs provided by the IGN
 151 (National Geographic Institute), sometimes produced by photogrammetric method. The time interval
 152 between the two series of aerial photographs is nearly 50 years (1947-2013) for the various territories
 153 (Table 3). This diachronic approach is classic (May and Heeps, 1985; Moore, 2000; Moore and

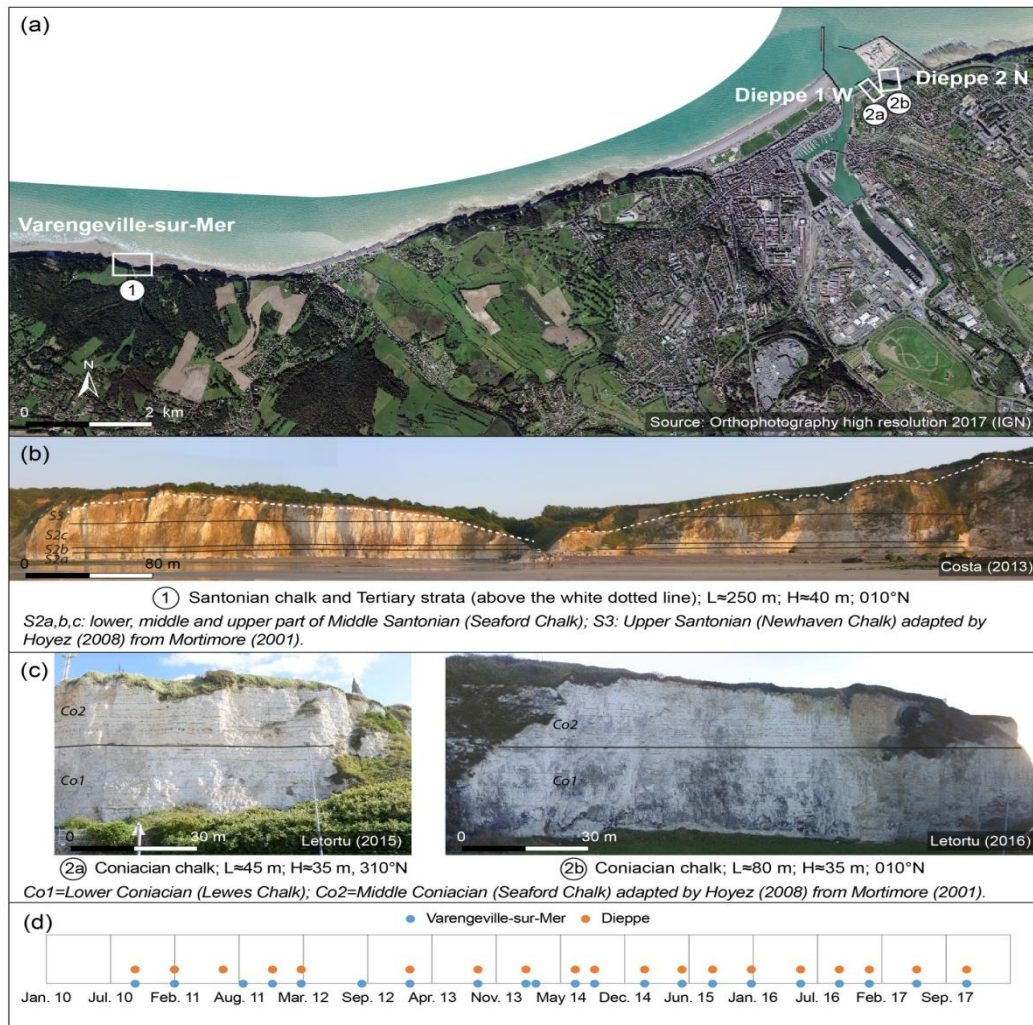
154 Griggs, 2002; Lahousse and Pierre, 2002; Hénaff *et al.*, 2002; Costa *et al.*, 2004; Marques, 2006;
155 Dornbusch *et al.*, 2008; Brooks and Spencer, 2010; Moses and Robinson, 2011; Letortu, 2013;
156 Cerema, 2015). After georeferencing and rectification of the images at from 1:10,000 to 1:20,000 scale
157 (Costa *et al.*, 2004; Letortu *et al.*, 2014; Lissak *et al.*, 2013; Maquaire *et al.*, 2013; Vioget, 2015;
158 Roulland *et al.*, accepted), the digitization of the coastline was carried out (cliff top for the Seine
159 Maritime, top and bottom for the Calvados cliffs). The margins of error of the results are not
160 negligible (+/- 0.50 m to +/- 4 m). Associated with these aerial photographs, we benefited from
161 airborne lidar data (RGE Alti- IGN) to provide a new layer of more accurate information (margin of
162 error +/- 20 cm) that completes the analysis. Finally, for the cliffs of Calvados, old documents
163 (cadastral registers) have been integrated. France has a single document, which is the cadastral map of
164 all the municipalities. The first of these cadastral registers, called Napoleonic, was established in the
165 19th century by order of Napoleon I. Carried out on a very large scale (from 1/1,000 to 1/2,500), this
166 document has been updated to this day. The principle is attractive, but these documents exclusively
167 express the limit of taxable parcels, which alone are perfectly mapped from one document to another.
168 Consequently, the correct setting of these plots is logical, but it does not in any way ensure, given the
169 danger of the measurement, the exact position of a very unstable steep slope of several tens of meters.
170 Even if the margins of error around the position of the shoreline are large, the loss of perfectly located
171 plots of land by erosion makes it possible to replace the cliff retreat rates obtained over a few decades
172 in a wider time period. In addition, the multiplicity of aerial images used for different dates (Table 3)
173 also makes it possible to provide initial information on the evolution rates of the studied cliffs.

174 **2.2/ Quantification at high resolution and frequency diachronic monitoring**

175 In order to participate in the current debate on (1) the evolution of the cliff face, for which it is
176 preferable, for analysis, to monitor the height or basal coastline (Lim *et al.*, 2005; Lim, 2014; Young *et al.*
177 *et al.*, 2009; Dewez *et al.*, 2007; 2013; Michoud *et al.*, 2014; Letortu *et al.*, 2015b; Rosser *et al.*, 2013) (2)
178 the rates of evolution (3) the processes responsible for the trigger of gravitational movements, a high
179 resolution and frequency diachronic monitoring is carried out on some sites by lasergrammetric (TLS)
180 and photogrammetric (SfM-MVS, *Structure-from-Motion - Multi-View-Stereo*) methods, completed on
181 two sites by several continuous or permanent GPS stations. This work was undertaken within the
182 framework of the SNO-Dynalit, but also SNO-OMIV.

183 Two sites are subject to these 3D monitoring in SNO Dynalit survey. These are the cap d'Ailly-Dieppe
184 site (Seine Maritime), which has been performed since 2010 (surveys 3 to 4 times a year), and the
185 Vaches Noires cliff near Villers-sur-Mer site since 2014 (surveys 3 to 4 times a year). On the third site
186 of the Villerville slow-moving landslide, the monitoring system is based on twenty-four cemented
187 benchmarks, three permanent GNSS receivers and several hydro-meteorological observation points
188 (Lissak *et al.*, 2014).

189 **The first site is Cap d'Ailly-Dieppe** (Fig. 3a). From October 2010 (Fig. 3d), surveys using terrestrial
190 laser scanning were carried out to monitor erosion on three chalk cliff faces with close lithological
191 characteristics. The active cliff of Varengeville-sur-Mer is along the cap d'Ailly (6 km from Dieppe)
192 on either side of the Petit Ailly dry valley (250 m long, 40 m high, facing 010°N, subvertical). The
193 abandoned cliffs of Dieppe are located on the right bank of the Arques river mouth, behind an
194 extension of the northeastern part of the harbor, land reclaimed from the sea. Dieppe 1 W (45 m long,
195 35 m high, facing 310°N, subvertical) became abandoned during the nineteenth century whereas
196 Dieppe 2 N (80 m long, 35 m high, facing 010°N, subvertical) became abandoned in the 1980s (Fig.
197 3a and c). The western cliff is in front of the quay for the Newhaven–Dieppe ferry crossings. The cliff
198 lithology in cap d'Ailly is made up with Santonian chalk, covered by a bed of clay and sand of
199 Paleogene period (due to the syncline prone to strata preservation), which are very prone to erosion
200 (Fig. 3b). The cliff section of Dieppe is made up of Coniacian chalk covered with residual flint
201 formation (Fig. 3c). Even if each facies within a stage can have some subtle resistance contrasts, the
202 Coniacian chalk is close to Santonian chalk (Laignel, 2003).
203

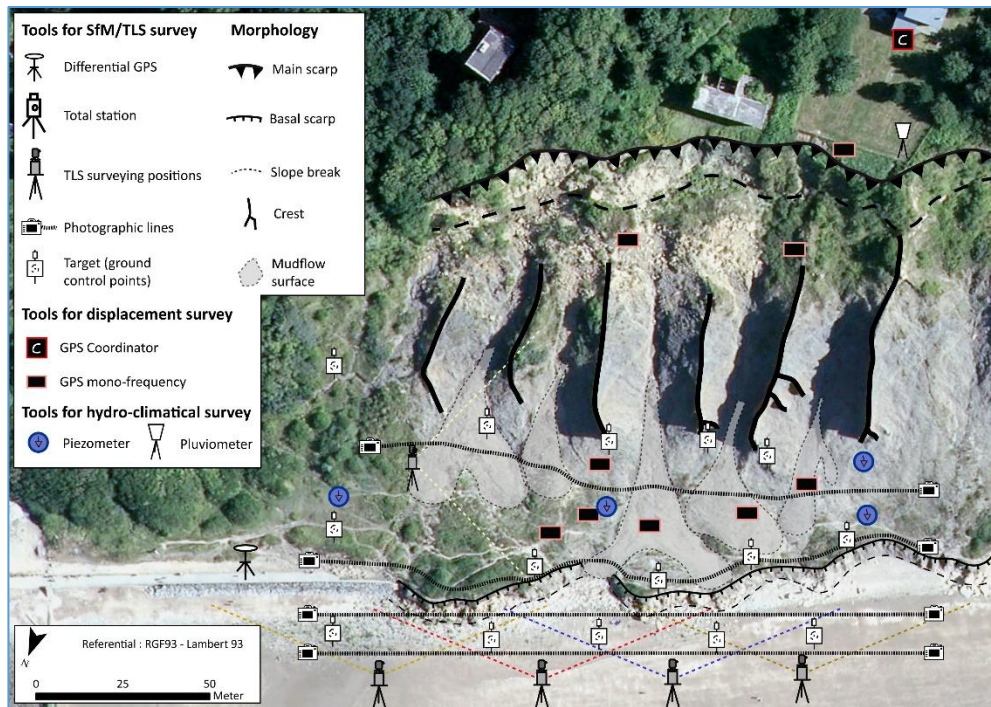


204
205

206 Figure 3: (a) Location of the sites; (b) Main characteristics of cap d'Ailly/Varengueville-sur-Mer
 207 site; (c) Main characteristics of Dieppe sites; (d) Terrestrial Laser Scanner (TLS) acquisition.

208

209 **The second site is Vaches-Noires coastal cliffs.** This site is located at the north-western part of the
 210 Pays-d'Auge region between Houlgate and Villers-sur-Mer (Fig. 4), and is armed by Jurassic
 211 limestone and clayed and marly formations. Their facies evolves under the action of continental and
 212 marine subaerial processes through the accumulation of deposits resulting from rotational landslides
 213 and/or mudflows at the base of the cliff which are then undermined by the sea (Maquaire *et al.*, 2013;
 214 Medjkane *et al.*, 2018). Since September 2014, on a 200 meters coastline, cliff is monitored using 3D
 215 models created by terrestrial laser scanner (3-4 surveys / year), terrestrial "Structure from Motion"
 216 photogrammetry (7-8 surveys / year) and Unmanned Aerial Vehicle (UAV) photogrammetry (2-3
 217 surveys / year). Nine single-frequency GPS have been installed on the site in order to continuously
 218 monitor the surface displacements (landslides and mudflows). A rain gauge and four piezometers are
 219 also installed on the site to have continuous rainfall values and oscillations of the water table.



220

221 Figure 4: Scheme of the measurement tools and equipment used for the monitoring of the “Vaches
222 Noires” cliffs

223 The **SNO-OMIV** survey is focused on the **Villerville slope** site. This site is affected by a deep-seated
224 rotational-translational complex landslide. It is monitored since the early 1980s, following the major
225 event of 1982 (Maquaire, 1990). In order to measure the seasonal displacements affecting the landslide
226 from upstream to downstream, 24 cemented landmarks were installed and their positions are regularly
227 measured by GNSS. Since 2009, this equipment is completed by the installation of 3 GNSS receivers
228 in the East part of the unstable area, which record their XYZ position every hour and provides a better
229 knowledge of the evolution rhythms (velocity, distance, direction and thresholds) (Lissak, 2012;
230 Lissak *et al.*, 2013). Groundwater fluctuations are observed across a network composed by a set of 20
231 piezometers and inclinometers, mainly distributed on the eastern two thirds of the landslide, which is
232 known as the most active area (Maquaire, 1990; Lissak, 2012; Lissak *et al.*, 2013). Among those
233 devices, six are continuously tracked with multiparameter sensors (temperature and depth), the others
234 are surveyed monthly with a contact gauge to highlight seasonal trends. Lastly, various hydro-
235 meteorological parameters are registered by meteorological stations that records rainfall, temperature,
236 solar radiation, wind speed and wind direction, nearby the unstable slopes at Villerville and on the
237 plateau located at Saint-Gatien-des-Bois from 5 kilometres of the cliffs.

238 Along the **Bessin cliff**, on a local scale, four sites are surveyed by TLS and terrestrial photogrammetry
239 SfM (4-5 times per year) since December 2017 in order to assess the rate of the retreat of the cliff base
240 following the triggering factors. These sites are representative of the diversity of the landslide (falls,
241 rotational and translational landslides ...) occurred in marly and limestone environments (Maquaire,
242 1990; Vioget, 2015). In addition, on a regional scale, the evolution of Bessin cliffs is study by
243 comparison of oblique aerial photographs taken since 1983 (thesis of Vincent Compain in progress).

244

245

246

247

248

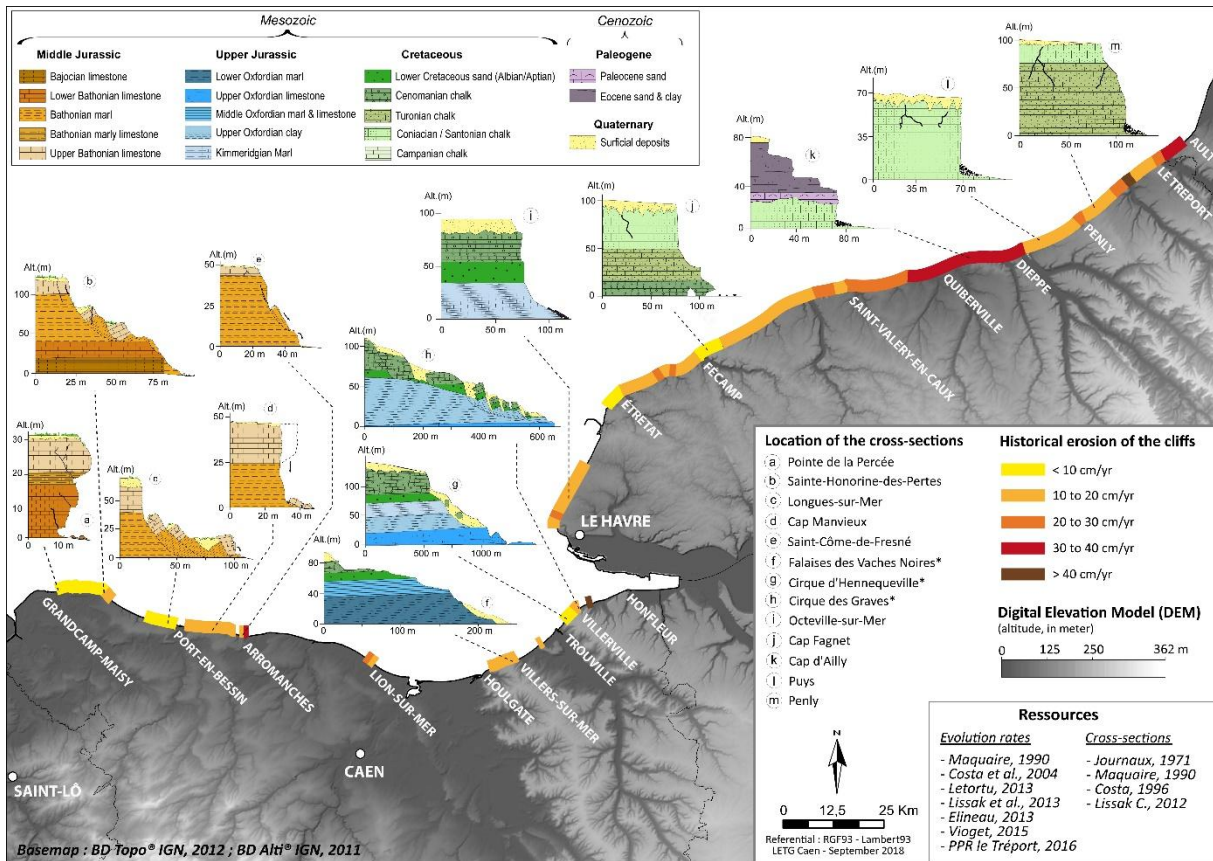
249 The TLS instrument used in this study is a RIEGL VZ-400 emitting a wavelength laser of 1,550 nm,
250 which records unique echo digitization (RIEGL Laser Measurement Systems, 2014). The laser beam
251 covers the environment with vertical scanning by an oscillating mirror and horizontal scanning by
252 rotating the head. The point cloud is therefore centered on the position of the scanner. To have
253 georeferenced data, the process of data acquisition requires additional equipment: target(s), a total
254 station or a DGPS. The total station or the DGPS station is used to register the point cloud acquired in
255 a relative coordinate system to an absolute coordinate system thanks to target(s) (RGF93/Lambert93,
256 EPSG:2154). Data processing has 4 steps: (1) georeferencing and point cloud alignment; (2) manual
257 point cloud filtering (vegetation, people, foreshore); (3) meshing using Delaunay triangulation and
258 generation of a 3D Digital Elevation Model (DEM); (4) creating a DEM of Difference (DoD).
259 Precision is the most important parameter in our monitoring, thus all the point clouds are fitted to a
260 selected reference point cloud using best fit alignment algorithms (Cloudcompare® or 3DReshaper®).
261 This adjustment reduces the error margin because it includes the TLS instrumental error (0.005 m at a
262 range of 100 m, RIEGL Laser Measurement Systems, 2014) and the cloud adjustment error (fitting)
263 only. To assess precision, fixed parts of the point cloud are compared using the usual data processing.
264 The precision in planimetry is 0.03 m for cap d'Ailly and Dieppe 2 N, 0.02 m for Dieppe 1 W and
265 Villers-sur-mer. The volume precision is $\pm 156 \text{ m}^3$ in cap d'Ailly (surface of $5,214 \text{ m}^2$), $\pm 9 \text{ m}^3$ in
266 Dieppe 1 W (434 m^2) and $\pm 30 \text{ m}^3$ in Dieppe 2 N ($1,018 \text{ m}^2$), and $\pm 3 \text{ m}^3$ in Villers-sur-Mer (111 m^2)
267 (Medjkane *et al.*, 2018). These improved resolutions, particularly over the whole cliff face, and the
268 higher frequency of acquisitions provide valuable information on ablation rates, spatial distribution,
269 temporalities and the processes and factors responsible for triggering of gravitational movements.

270 The models obtained by SfM processing followed the method presented in Medjkane *et al.* (2018).
271 The processing steps, carried out with Agisoft Photoscan, can be summarized as follows: (1) Image
272 matching and orientation of cameras; (2) densification of the 3D point cloud; (3)
273 triangulation/meshing of the point cloud; (4) texturing of the model; (5) creation of a DoD. The same
274 targets used to georeference lasergrammetric models were used in photogrammetric models.
275 Photographs were obtained with an advance grade camera to further improve model precision: Nikon
276 D810 (36 million pixels, sensor size 36x24 mm) and a Sigma 35 mm fixed optics. Finally, to assess
277 precision, the accuracy of control points on the model was compared with the precisely measured
278 GCPs by calculating the RMSE (*Root Mean Square Error*, Eltner *et al.* 2016, Kaiser *et al.* 2014).
279

280 **3/ Results**

281 **3.1/ Historical approach for all Norman sedimentary cliffs**

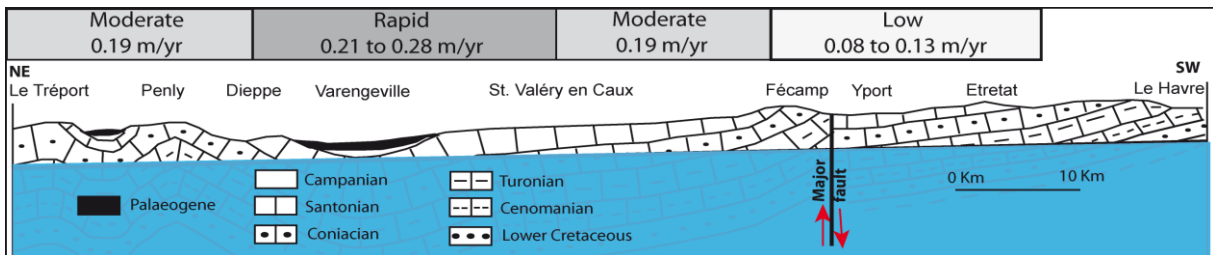
282 The study of the Norman sedimentary cliffs shows that their retreat is decimetric, from 0.1 to 0.5 m/yr
283 during the last decades. These values are in line with the literature (Woodroff, 2002). The spatial
284 variations of the cliff retreat rates, at the scale of Normandy, can be explained by geological structure
285 from which the cliffs were formed) (Fig. 5). However, the differences are not excessive while various
286 materials, of significantly different resistance, are exposed (limestones, chalks, marls, clays). The
287 greatest variations of retreat appear for the cliffs of Seine Maritime which are nevertheless carved in
288 materials, *a priori* more homogeneous, Cretaceous chinks.



289
290 Figure 5: Synthesis of historical rates retreat of the Normandy sedimentary cliffs (in cm/year).

291 **Example of lithodependance: the chalk cliff of Seine Maritime**

292 Various authors have proposed cliff typologies that relate profile, resistance and disposition of rocks
 293 (Guilcher, 1954; Trenhaile, 1987; Maquaire, 1990; Costa, 1997; Woodroffe, 2002; Senfaute et al,
 294 2009; Dornbusch et al, 2008; Kennedy et al, 2014). These classifications sometimes make it possible
 295 to deduce the effectiveness of the marine and continental processes involved (Emery and Kuhn, 1982;
 296 Kuhn and Prüfer, 2014). Behind a lithological homogeneity that is only apparent, the variability of the
 297 facies of the Seine Maritime chalk (Pomerol *et al.*, 1987; Mortimore *et al.*, 2004; Lasseur, 2007) very
 298 clearly influences the modalities and evolution rates of the Seine-Maritime cliffs. Photogrammetry
 299 analyses were carried out to quantify the retreat of chalk cliffs. The 1966 and 1995 vertical aerial
 300 photographic surveys (1:10,000) from the French National Geographic Institute have been used (Costa
 301 *et al.*, 2001; 2004). The mean retreat rate of the entire shoreline under study is approximately 6 m
 302 between 1966 and 1995, which yields a rate of 0.21 m/yr. This average rate, however, masks a very
 303 high spatial variability of cliff retreat (Fig. 6).



304
305 Figure 6: Relationship between chalk rates cliff retreat and lithology (from Costa et al. 2001; 2004;
 306 Letortu *et al.*, 2014).
 307 In fact, the analysis allows three distinct areas to be distinguished: (i) an area of low retreat rate (0.8 to
 308 0.13 m/yr) between Antifer and Fécamp; (ii) an area of moderate retreat rate (approximately 0.19

309 m/yr) between Fécamp and Saint-Valéry-en-Caux, and between Dieppe and Le Tréport; (iii) an area of
310 rapid retreat (0.21 to 0.28 m/yr) between Saint-Valéry-en-Caux and Dieppe (Costa *et al.*, 2001; 2004;
311 Letortu *et al.*, 2014).

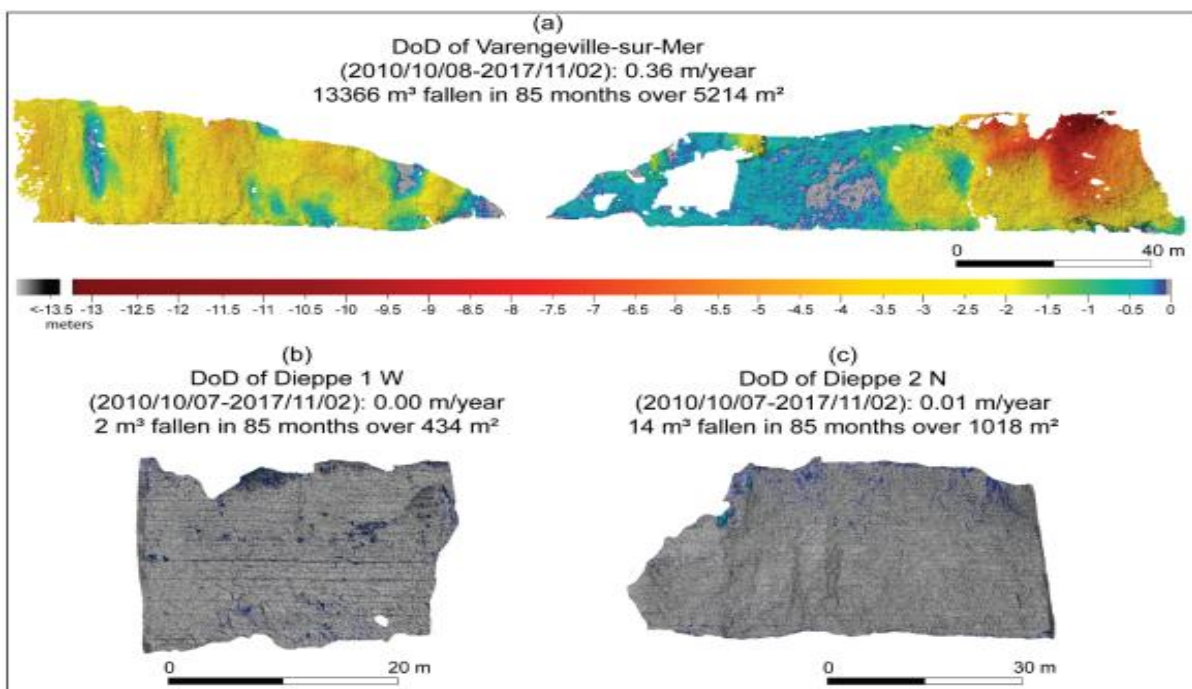
312

313 3.2/ Contributions of high resolution and frequency measurements

314 Ablation rates and spatial distribution of the cliff face evolutions

315 For fast retreating cliffs, the emergence of techniques such as airborne or terrestrial lidars, terrestrial or
316 UAV photogrammetry have made it possible to better estimate cliff retreat rates by integrating a
317 fundamental dimension, the cliff face (Lim *et al.*, 2005; Rosser *et al.*, 2005; Young and Ashford, 2006;
318 Costa *et al.*, 2001; 2004; Lahousse and Pierre, 2002; Dewez *et al.*, 2007; 2013; Young *et al.*, 2009;
319 Lim *et al.*, 2010; Olsen *et al.*, 2011; Letortu *et al.*, 2015b; Michoud *et al.*, 2014; Kuhn and Prüfer,
320 2014; Giuliano *et al.*, 2015; Rosser *et al.*, 2013).

321 This work (Fig. 7), carried out approximately every 3-5 months on active and abandoned chalk cliffs
322 (cap d'Ailly and Dieppe, respectively), but with similar lithology, shows that over the period studied
323 (2010-2017): (1) The ablation rate evaluated by TLS on active cliffs over a period of 7 years
324 corroborates that established by photo-interpretation (observed over nearly 50 years), i.e. around 36
325 cm/year for the cap d'Ailly and almost zero for the abandoned cliffs of Dieppe; (2) in 7 years, the
326 entire front of the active cliff is affected by debris or mass movements; (3) scree movements (debris
327 falls) represent 100% of the evolution of the abandoned cliff faces (for the moment!), while they
328 represent 2% of the total retreat of the active cliff of cap d'Ailly. This quantification highlights the
329 poor contribution of debris falls, and explains in a more detailed way the first assessments made on the
330 same Norman chalk cliffs and East Sussex (Lageat *et al.*, 2006; May and Heeps, 1985); (4)
331 Abandoned cliffs have evolved up to 36 times more slowly than active one, highlighting the
332 importance of marine actions in the active cliff retreat (Letortu *et al.*, 2015b).

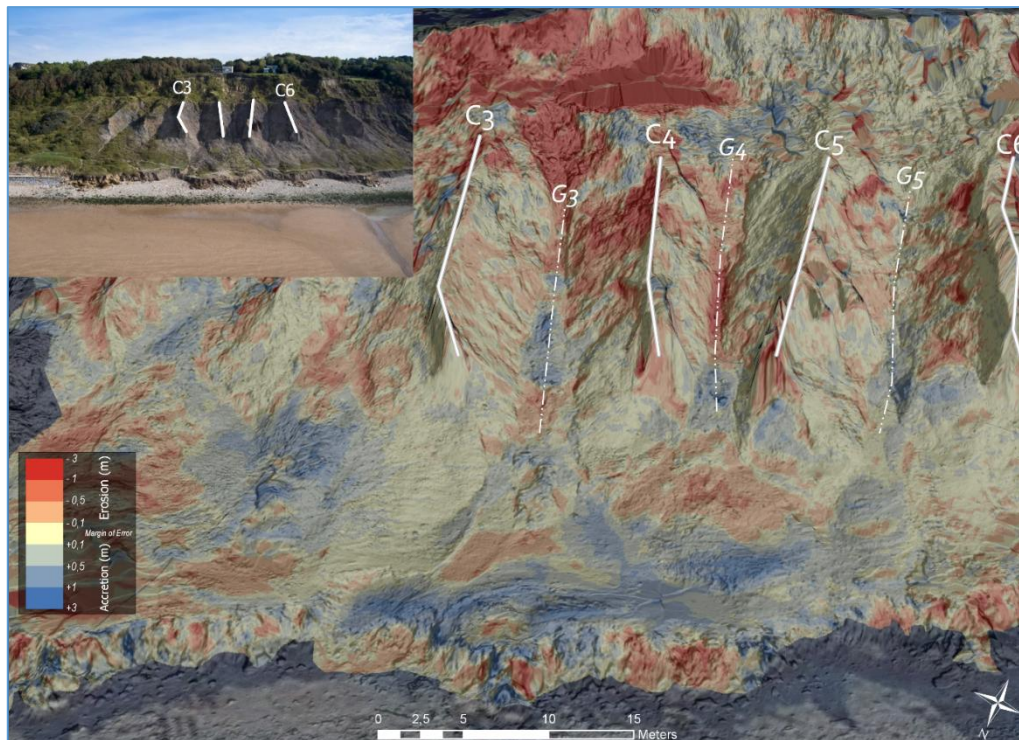


333

334 Figure 7: Erosion results of DoD over 7-years of monitoring of “cap d’Ailly/Varengueville-Dieppe”
335 site.

336 For the “Vaches noires” cliffs, the TLS differential model (March 2015 and October 2017) clearly
337 identifies erosion areas (red color) and accretion areas (blue color) (Fig. 8) at high spatial resolution.
338 The main eroding areas are the upstream scarp, the flanks of the interfluvial ridges, and the basal scarp.

339 Those in accumulation are visible at the outlet of the gullies and very locally at the top of the basal
 340 scarp. However, in detail, we note that the erosion and accumulation sectors follow one another
 341 spatially in the gullies, at their outlet and at the level of the basal scarp. These values reveal the
 342 seasonal activity of the cliffs of the “Vaches Noires” with a contribution of materials upstream of the
 343 cliffs and the finest elements that will then be partially cleaned and swallowed by the sea. After these
 344 observations, the high temporal frequency survey allowed to assess the different accumulated / eroded
 345 volumes according to the processes and associated morphologies (ablation zone and accumulation
 346 zone) between the different dates in order to better understand the seasonal temporality and the role
 347 and the weight of each controlled factors (sea erosion and groundwater elevation) (Thomas Roulland
 348 thesis in progress).



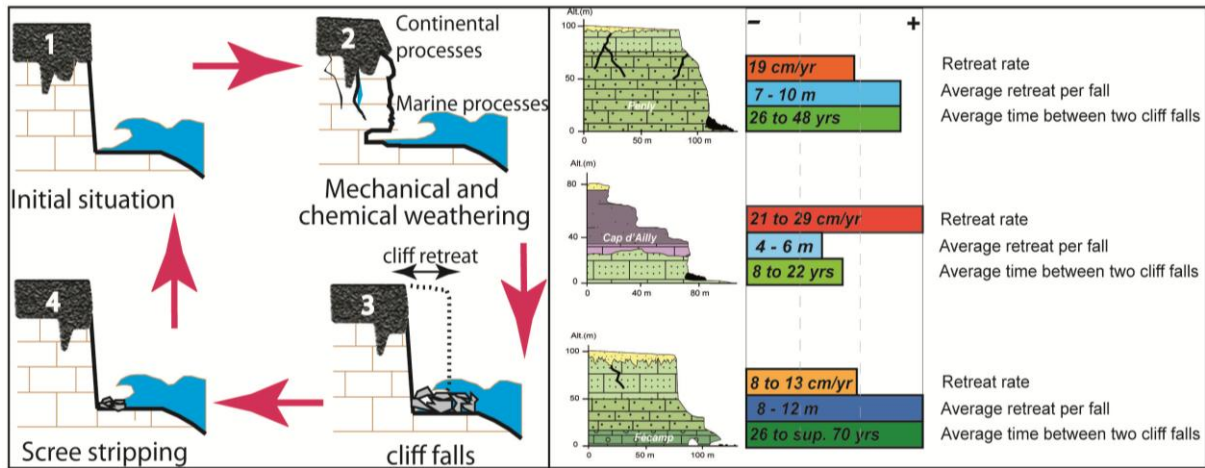
349
 350 Figure 8: Erosion and accretion areas: TLS differential model of “Vaches noires” cliffs (March 2015 -
 351 October 2017)

352 4/ Discussion

353 4.1/ Rhythms of evolutions

354 The identification of several sectors with distinctive retreat rates raises questions about the causes of
 355 this spatial distribution of the cliff retreat rates (especially its relation to the outcropping of different
 356 chalk strata), and more, the temporalities between two cliff collapses at the same location (Evrard et
 357 Sinelle, 1980; Trenhaile, 1987; 2011; Sunamura, 1992; Prager *et al.*, 2008; Kennedy *et al.*, 2014). The
 358 knowledge of the cliffs evolution rhythms is as fundamental as that of their rates, especially in the
 359 context of the timing of the movement of properties and people threatened by the decline. As the
 360 Figure 9 shows for the chalk cliffs of Seine Maritime, the sectors with “low” and “moderate” retreat,
 361 are affected by infrequent but voluminous rockfalls (Costa 1997; Costa et al. 2003; 2004; Letortu
 362 2013), and correspond to cliff foot cut into Turonian, Cenomanian, and even Coniacian outcrops
 363 (Antifer/Fécamp ; Fécamp/Saint-Valéry-en-Caux ; Dieppe/Le Tréport). By contrast, the rapidly
 364 retreating sectors, affected by frequent but less voluminous rockfalls, correspond to Santonian and
 365 Campanian outcrops (Saint-Valéry-en-Caux/Dieppe).

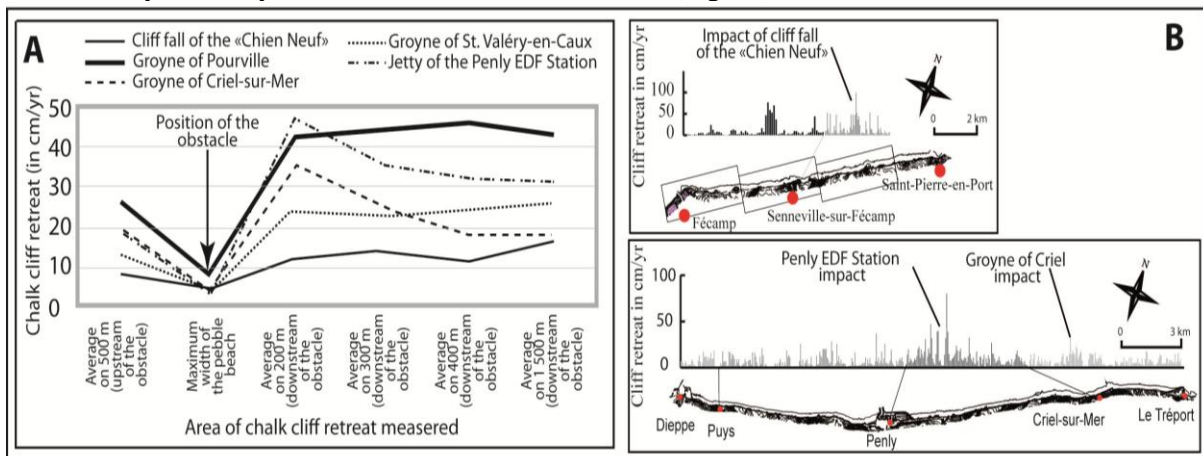
366



367 Figure 9: Cliff retreat, average retreat per fall and average time between two cliff falls for cliffs chalk
368 of Seine Maritime.

369 Even within each of these coastal sections, important variations do exist. These sharp variations are
370 linked with the influence of cliff collapses or anthropogenic obstacles, such as harbour arms or major
371 groynes that disrupt the gravel transit from the south-west to the north-east. Then down current from
372 these obstacles, the cliff retreat can be multiplied by 2 (Costa *et al.*, 2006). These observations are
373 confirmed by the analysis of the retreat at 50 m intervals (Fig. 10).

374



375 Figure 10: Impact of major cliff falls or anthropogenic obstacles on chalk cliff retreat of Seine
376 Maritime (A), and some examples of measures at 50 m intervals (B).

377 For the **“Vaches Noires”** cliffs, by comparing old documents (terrier plan, land register map, aerial
378 photographs, postcard photography) and more contemporary data (orthophotographs, satellite images,
379 dGPS surveys, LIDAR survey) between 1759 and 2016 (257 years), the results show a marked decline
380 in the main scarp estimated at - 0.39 m/year, but also an average annual decline of - 0.27 m/year
381 between 1837 and 2016 (179 years). The secondary scarp declined more modestly by - 0.23 m/year
382 between 1759 and 2016 (257 years), then by - 0.48 m/year over the period 1837 and 2016 (179 years).
383 The basal scarp has a more contrasted evolution, with some sectors in erosion, others in progradation,
384 and some sectors without significant evolution (or included in the margins of error). The erosion
385 values are generally between - 0.02 m/year to - 0.15 m/year between the different periods. The
386 progradation values range from + 0.02 m/year to + 0.15 m/year, often included in front of the locality
387 "Hermitage". Comparison with the average evolution rates (in m/year) of other Normandy clay and
388 marl cliffs (ranging from -0.15 m/year to -0.30 m/year) showed that the foot of the basal scarp suffered
389 a slight overall decline. These studies showed that nuances needed to be made in the evaluation of
390 shorter time step velocities due to the reactivation and progression of major landslides on the foreshore
391 that alter the coastline. In the cliffs of the “Vaches Noires”, this is visible in the area known as
392 "l'Hermitage" where a large landslide occurred between 1837 and 1947, causing the main scarp to

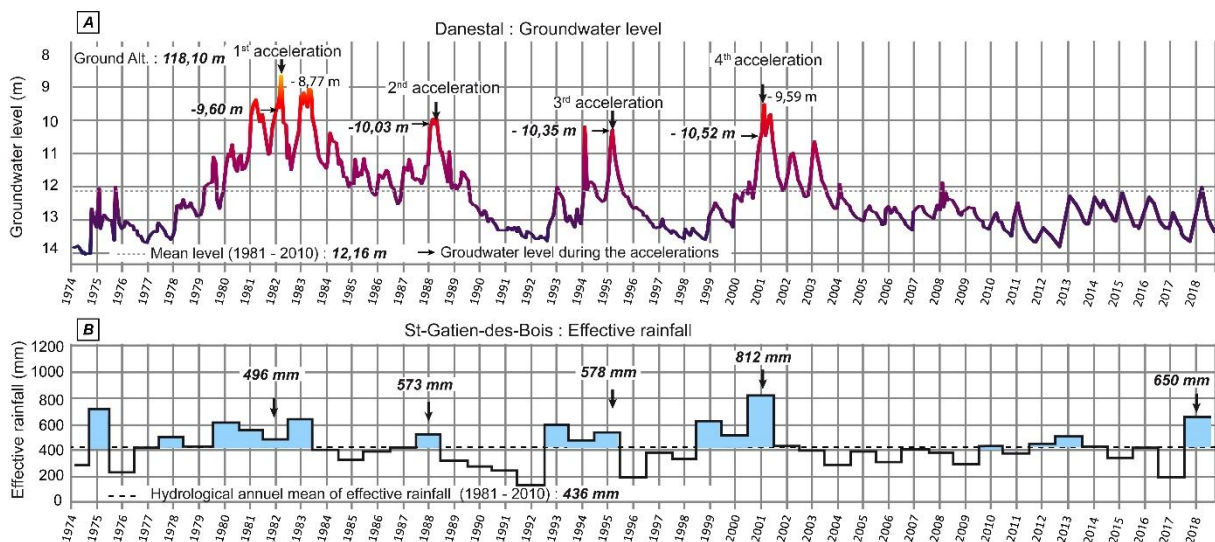
393 retreat by more than 120 m and the coastline to advance by more than 50 m (Maquaire *et al.*, 2013;
 394 Roulland *et al.*, in press).

395 Thus, on sectors with cliffs evolving by landslides and mudflows, nuances in the evolutions must be
 396 made according to the sectors and according to the periods considered. The evolution calculated over a
 397 long period is probably more significant when taking into account the "cycle" of evolution of the cliff.
 398 For marl cliffs of different configurations, evolution can occur within cycles of 30 to 40 years in
 399 London clays (Hutchinson, 1973), or of a hundred years in the Gault clay cliffs of Dorset (Brunsden
 400 and Jones, 1980) where the activation of summit flows depends largely on the retreat of the lower part
 401 of the cliff (Pierre, 2005). Thus, for the "Vaches Noires" cliffs, the duration of the "cycle" to be taken
 402 into account would be at least around 250 to 300 years to be able to set a long-term evolutionary trend
 403 of decline.

404 **4.2/ Factors responsible for triggering gravitational landslides (rockfall, slide, debris fall) and**
 405 **thresholds**

406 The cross-referencing of multi-date and multi-document data as well as that of some agents as erosion
 407 processes can provide information about the factors responsible for triggering gravitational landslides.
 408 At the **SNO-OMIV landslide of Villerville**, the link was clearly established between efficient rainfall,
 409 groundwater level and displacements of the unstable slopes (Maquaire, 1990; Lissak *et al.*, 2009;
 410 Lissak, 2012). Efficient rainfall increase the roof level of the groundwater until it exceed a threshold
 411 rain quantity, considered in the literature as the main triggering factor of worldwide landslides
 412 (Zezere, 2002; Zezere *et al.*, 2015; Guzzetti *et al.*, 2008; Peruccacci *et al.*, 2017). The link
 413 intensity/duration has a particular impact on the overtaking of this threshold (Zezere *et al.*, 2015).

414 In order to highlight the relationship between rain, groundwater and displacement of the Villerville
 415 deep-seated landslide, long-term chronicles of data should be used (Fig. 11). To this end, data from a
 416 piezometer of the national network located in Danestal (in the hinterland, on the Pays d'Auge plateau)
 417 were crossed-analysed with efficient rainfall data measured at the Météo-France weather station of
 418 Saint-Gatien-des-Bois (located 5 km backwards the landslide). Then, those chronicles were linked to
 419 the major events known which affected this great coastal landslide.

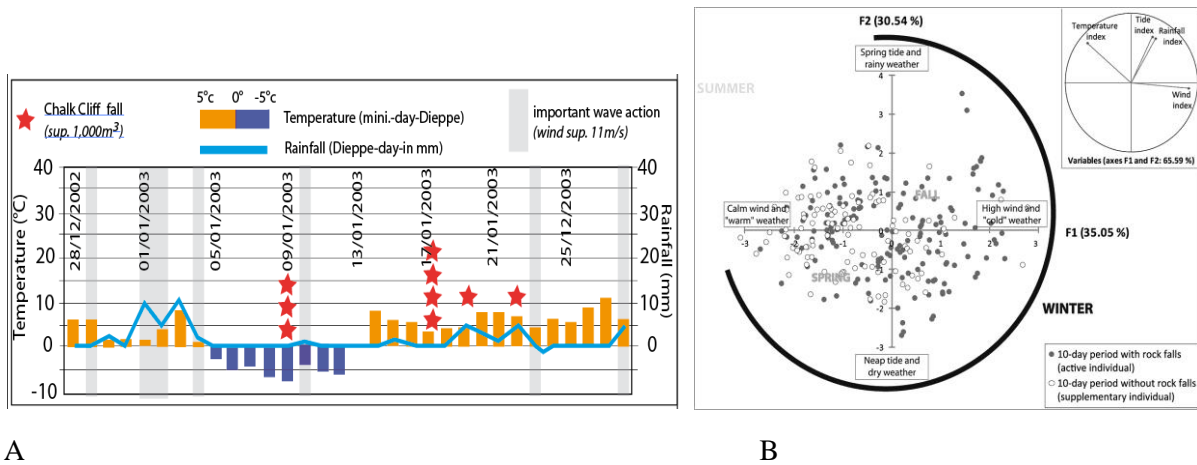


420
 421 Figure 11: Evolution of the groundwater level of the Danestal well and of the effective annual rainfall
 422 of the St-Gatien-des-Bois climatic station from 1974 to 2018

423 This correlation analysis, initially expressed by Lissak (2012), revealed a small-scale causal
 424 relationship between the hinterland groundwater level and the four major accelerations observed on
 425 the coast (Fig. 11). From this observation, a regional warning threshold have been proposed in cases in

426 which the piezometer of Danestal exceed a depth of 11m/GL and the effective rain on a 4-months-
427 period is over 250 mm (Lissak *et al.*, 2013).

428 **For the chalk cliffs of Seine Maritime**, determination of the triggering factors of rock falls is more
429 difficult. Based on a census of 331 chalk cliff rock falls collected weekly between 2002 and 2009 from
430 Veules-les-Roses to Le Treport the relationship between dates of cliff rock falls and external factors
431 commonly agreed as triggering (rainfall, temperature variations, tide and wind) is studied (Fig. 12).
432 The combination of multivariate statistical and empirical analyses indicates (Letortu *et al.*, 2015a) that,
433 (1) the high rainfall are an essential triggering factors and especially the most massive chalk rock falls
434 (mostly larger than 10,000 m³) (confirmed studied of Pierre and Lahousse, 2006; Duperret *et al.*, 2002;
435 2004; 2005), (2) but also the freeze/thaw cycles which are responsible for scree production phenomena
436 (individual particles), (3) marine factors are not negligible but their influence is difficult to quantify
437 because rock falls of small volumes may be quickly removed during a turbulent period. However, the
438 contribution of each factor to triggering is difficult to determine because of combinations of factors
439 (84 % of 331 cases), relays of processes and hysteresis phenomena. In view of these first results, it is
440 still presumptuous to predict the location and time of triggering of rock falls. However, the statistical
441 and naturalistic approaches adopted and the observations made in this study are from an original
442 database, and constitute a real starting point for the prediction and prevention of the hazard of coastal
443 chalk cliff rock falls.



444
445 A

446 Figure 12: Example of relationship between cliff falls inventoried and external factors shows
447 combinations and relays of processes (A), and multivariate statistical analyses (PCA) of 331 chalk
448 cliff rock falls (Letortu *et al.*, 2015a) of Seine Maritime (B).

449 Conclusion

450 The retreat rates of the sedimentary cliffs of Normandy are about 20-30 cm/year. These values are in
451 line with what is generally observed for this type of geology (Woodroff, 2002; Dunrbush *et al.*, 2008;
452 Mooses and Robinson, 2011; Kennedy *et al.*, 2017). Spatial disparities are due to lithological
453 variations (outcrop less resistant at the foot of cliffs), but also and above all to the existence of
454 obstacles to coastal drift (structures or cliff falls) which considerably and locally increase the retreat
455 rates. These values are also comparable to what has been observed on the English coasts for similar
456 materials (Durnbush *et al.*, 2008) while the orientation towards swells is different. However, beyond
457 the lithological variations there may be other factors that explain the spatial variation in retreat rates.
458 Among these factors not exposed in this work are the width of the platform, the height of the cliff, the
459 width of the beaches at the foot of the cliffs, the intensity of the fracturing of the rocks, the presence of
460 more or less important groundwater...

461 This work also shows the interest of diachronic analysis using a multisource and multitemporal
462 approach (comparison of historical documents of modest precision, but allowing observation over

463 large areas with high frequency and high resolution data, allowing the cliff face to be studied locally).
464 This work provides information on the "periodicities" of the evolution of the various cliffs that are
465 essential for the temporal management of the movement of goods and people.

466 The high frequency and high resolution monitoring carried out as part of SNO-Dynalit and SNO-
467 OMIV greatly improves the knowledge of these sites. Even if the monitoring is carried out only in
468 fairly small areas, it allows to finely spatialize the evolutions, especially on the cliff face. It makes it
469 possible to distinguish between screes and mass movements, to quantify the production of debris
470 brought to the sea. However, the development of these new techniques (laser and photogrammetry) is
471 recent (a decade). The results therefore have a limited temporal representativeness. To be exhaustive,
472 high-resolution data will have to be acquired over the entire cliff evolution periodicity ("evolution
473 cycle"), which for some of them is at least two decades. Similarly, the frequency of surveys should be
474 well above 3-4 per year to define the agents and processes responsible for weathering cliffs or
475 triggering gravity movements. It is also for these reasons that it is very difficult to estimate the impact
476 of climate change and sea level rise on cliff recession rates. Moreover, the extent of anthropization on
477 coastal dynamics in recent decades masks the possible influence of these global changes.

478 This work also shows the importance of setting up observatories for long-term monitoring such as
479 INSU's SNO-Dynalit and SNO-OMIV, or INEE's "workshop zones" ("Zones Ateliers" of National
480 Institute on Ecology and Environment studies).

481 **Acknowledgements**

482 This research was supported by several projects: the project "Developing Geomorphological mapping
483 skills and datasets in anticipation of subsequent Susceptibility, Vulnerability, Hazard and Risk
484 Mapping" funded by the EUR-OPA European Major Hazards Agreement of the Council of Europe;
485 the ANR project "RICOCHET: multi-Risk assessment on Coastal territory in a global CHange
486 context" funded by the French Research National Agency (ANR-16-CE03-0008); the project "RAiv
487 Cot: flood and storm surge Risk and Hazard of coastal towns : quantitative and virtual reality approach
488 funded by Normandy Regional Council and by Fondation de France; the project "Teledetac:
489 Télédétection par DronE du Trait de Côte" funded by Normandy Regional Council; the project
490 "TOSCA CNES – SWOT 2013 and SWOT COTEST 2018 funded by the CNES.

491 **References**

- 492 Augris, C.; Clabaut, P.; Costa, S.; Gourmelon, F., and Latteux, B., 2004. *Évolution morpho-*
493 *sédimentaire du domaine littoral et marin de la Seine-Maritime*. Collection « Bilan and
494 prospectives », Ifremer, 158p.
- 495 Benabdellouahed, M.; Dugue, O.; Tessier, B.; Thinon, I.; Guennoc, P., and Bourdillon, C., 2014.
496 Nouvelle cartographie du substratum de la baie de Seine et synthèse géologique terre-mer : apports de
497 nouvelles données sismiques et biostratigraphiques. *Géologie de France*, 1, 21-45.
- 498 Bignot, G., 1971. Carte géologique de Dieppe (ouest), BRGM, scale 1:50,000, 1 sheet.
- 499 Bird, E., 2000. *Coastal Geomorphology. An introduction*. Chichester: John Wiley, XV, 322p.
- 500 Brooks, S.M. and Spencer, T., 2010. Temporal and spatial variations in recession rates and sediment
501 release from soft rock cliffs, Suffolk coast, UK. *Geomorphology*, 124, 26–41.
- 502 Brunsdon, D. and Jones, D. K. C. 1980. Relative time scales and formative events in coastal landslide
503 systems. *Zeitschrift fur Geomorphologie*, 4, 1-19.

- 504 Brunsden, D., and Lee, E.M. 2004. Behaviour of coastal landslide systems: an interdisciplinary view.
505 *Zeitschrift für Geomorphologie*, 134, 1-112.
- 506 CEREMA and Ministère de l'Écologie, du Développement Durable et de l'Énergie, 2015. *Développer*
507 *la connaissance et l'observation du trait de côte - Contribution nationale pour une gestion intégrée.*
508 24p.
- 509 CEREMA. In press. *Dynamiques et évolution du littoral. Fascicule 3 : synthèse des connaissances du*
510 *cap d'Antifer au cap de la Hague.* Margny-Lès-Compiègne, Collection « Connaissances », Edition
511 Cerema, 700p.
- 512 Costa, S., 1997. Dynamique littorale et risques naturels : l'impact des aménagements, des variations du
513 niveau marin et des modifications climatiques entre la Baie de Seine et la Baie de Somme. Paris,
514 France: Paris I Panthéon Sorbonne, Thèse de doctorat en Géographie, 327 p.
- 515 Costa, S.; Delahaye, D.; Freire-Diaz, S.; Davidson, R.; Di-Nocera, L., and Plessis, E., 2004.
516 Quantification of the Normandy and Picardy chalk cliff retreat by photogrammetric analysis.
517 *Engineering Geology, Special Publications*, 20, 139-148.
- 518 Costa, S.; Freire-Diaz, S., and Di-Nocera, L., 2001. Le littoral haut normand et picard : une gestion
519 concertée. *Annales de Géographie*, 618, 117-135.
- 520 Costa, S.; Henaff, A., and Lageat, Y., 2006. The gravel beaches of North-West France and their
521 contribution to the dynamic of the coastal cliff-shore platform system. *Zeitschrift für Geomorphology.*
522 *Suppl.-Vol.*, 144, 199-194.
- 523 Costa, S.; Lageat, Y.; Henaff, A.; Delahaye, D., and Plessis, E. 2003., Origine de la variabilité spatiale
524 du recul des falaises crayeuses du nord-ouest du Bassin de Paris. L'exemple du littoral haut normand
525 (France). *Hommes et Terres du Nord*, 2003(1), 22-31.
- 526 Davis, R.A. Jr, and Fitzgerald, D.M., 2003. *Beaches and Coasts*, Oxford: Blackwell Publishing, 419p.
- 527 Dewez, T. J. B.; Rohmer, J.; and Closset, L., 2007. Laser survey and mechanical modeling of chalky
528 sea cliff collapse in Normandy, France. In: Mc Innes, R., Jakeways, J., Fairbanks, H. and Mathie, E.
529 (Eds.), *Proceedings of Landslides and Climate Change, Challenges and Solutions* (Isle of Wight,
530 England), pp. 281-288.
- 531 Dewez, T. J. B.; Rohmer, J.; Regard, V., and Cnudde, C., 2013. Probabilistic coastal cliff collapse
532 hazard from repeated terrestrial laser surveys: case study from Mesnil Val (Normandy, northern
533 France). In: Conley, D.; Masselink, G.; Russel, P., and O'Hare, T. (Eds), *Proceedings 12th*
534 *International Coastal Symposium* (Plymouth, England). *Journal of Coastal Research*, Special Issue
535 No. 65, pp. 702-707.
- 536 Dornbusch, U.; Robinson, D.A.; Moses, C.A., and Williams, R.B.G., 2008. Temporal and spatial
537 variations of chalk cliff retreat in East Sussex, 1873 to 2001. *Marine Geology*, (249), 271-282.
- 538 Dugué, O., 1989. Géodynamique d'une bordure de massifs anciens. La bordure occidentale du bassin
539 anglo-péruvien au Callovo-Oxfordien. Pulsations épirogéniques et cycles eustatiques. Caen, France:
540 Université de Caen, Thèse de doctorat.
- 541 Dugué, O.; Fily, G., and Rioult, M., 1998. *Le Jurassique des Côtes du Calvados. Biostratigraphie,*
542 *sédimentologie, paléocéologie, paléogéographie et stratigraphie séquentielle.* Le Havre, France:
543 Bulletin trimestriel société géologique Normandie et Amis Muséum du Havre, 85(2), 132p.
- 544 Duperret, A.; Genter, A.; Martinez, A., and Mortimore, R. N., 2004. Coastal chalk cliff instability in
545 NW France: role of lithology, fracture pattern and rainfall. In: Mortimore, R.N., and Duperret, A.

- 546 (eds.), *Coastal Chalk Cliff Instability*, London, Geological Society, *Engineering Geology* Special
547 Publication, 20, pp. 33-55.
- 548 Duperret, A.; Genter, A.; Mortimore, R. N.; Delacourt, B., and De Pomerai, M. R., 2002. Coastal rock
549 cliff erosion by collapse at Puys, France: The role of impervious marl seams within chalk of NW
550 Europe. *Journal of Coastal Research*, (18), 52-61.
- 551 Duperret, A.; Taibi, S.; Mortimore, R. N., and Daigneault, M., 2005. Effect of groundwater and sea
552 weathering cycles on the strength of chalk rock from unstable coastal cliffs of NW France.
553 *Engineering Geology*, (78), 321-343.
- 554 Elineau, S., 2013. Le risque naturel côtier sur la communauté d'agglomération du Havre (Haute-
555 Normandie) : Une évaluation des aléas. Le Havre, France: Université du Havre, Thèse de doctorat.
- 556 Eltner, A.; Kaiser, A.; Castillo, C.; Rock, G.; Neugirg, F. and Abellán, A. (2016). Image-based surface
557 reconstruction in geomorphometry - merits, limits and developments. *Earth Surface Dynamics*, (4),
558 359-389.
- 559 Emery, K.O., and Kuhn, G.G., 1982. Sea cliffs: their processes, profiles, and classification. *Geol. Soc.*
560 *Am. Bull.*, 93, 644–654.
- 561 Evrard, H., and Sinelle, C., 1980. Stabilité des falaises du Pays de Caux. Le Petit-Quevilly, France:
562 Centre d'étude technique de l'Équipement, Laboratoire Régional des Ponts et Chaussées, 88p.
- 563 Genter, A.; Duperret, A.; Martinez, A.; Mortimore, R.N., and Vila, J.-L., 2004. Multiscale fracture
564 analysis along the French chalk coastline for investigating erosion by cliff collapse. *In*: Mortimore,
565 R.N., and Duperret, A. (eds.), *Coastal Chalk Cliff Instability*, London, Geological Society,
566 *Engineering Geology* Special Publication, 20, pp. 57–74.
- 567 Giuliano, J., 2015. Erosion des falaises de la région Provence-Alpes-Côte d'Azur : évolution et origine
568 de la morphologie côtière en Méditerranée : télédétection, géochronologie, géomorphologie. Nice,
569 France: Université de Nice, Thèse de doctorat, 443p.
- 570 Gómez-Pujol, L.; Pérez-Alberti, A.; Blanco-Chao, R.; Costa, S.; Neves, M., and Río, L.D., 2014. The
571 rock coast of continental Europe in the Atlantic. *In*: Kennedy, D.M.; Stephenson, W.J., and Naylor,
572 L.A. (eds.), *Rock Coast Geomorphology: A Global Synthesis*, London, Geological Society, *Book*, 40,
573 pp. 77–88.
- 574 Guilcher, A., 1964. *Coastal and Submarine Morphology*. London: Methuen and Co, 274 pp.
- 575 Guzzetti, F.; Peruccacci, S.; Rossi, M., and Stark, C.P., 2008. The rainfall intensity–duration control of
576 shallow landslides and debris flows: an update. *Landslides*, 5(1), 3- 17.
577 <https://doi.org/10.1007/s10346-007-0112-1>.
- 578 Hénaff, A.; Lageat, Y.; Costa, S., and Plessis, E., 2002. Le recul des falaises crayeuses du Pays de
579 Caux: détermination des processus d'érosion et quantification des rythmes d'évolution/Retreat of
580 chalk cliffs in the Pays de Caux: processes and rates. *Géomorphologie Relief Process. Environ.* 8,
581 107–118.
- 582 Hutchinson, J.N., 1973. The response of London Clay cliffs to different rates of toe erosion. *Geologica*
583 *Applicata e Idrogeologica*, 8, 221 – 239.
- 584 Juignet, P., and Breton, G., 1992. Mid-Cretaceous sequence stratigraphy and sedimentary cyclicity in
585 the western Paris Basin. *Paleogeography, Paleoclimatology, Paleoecology*, 91, 197-218.

586 Juignet, P., 1974. La transgression crétacée sur la bordure orientale du Massif armoricain. Caen,
587 France: Université de Caen, Thèse de doctorat.

588 Kaiser, A.; Neugirg, F.; Rock, G., Müller, C., Haas, F.; Ries, J., and Schmidt, J., 2014. Small-scale
589 surface reconstruction and volume calculation of soil erosion in complex moroccan gully morphology
590 using Structure-from-Motion. *Remote Sensing*, 6, 7050-7080.

591 Kennedy, D.M.; Coombes, M.A., and Mottershead, D.N., 2017. The temporal and spatial scales of
592 rocky coast geomorphology: a commentary. *Earth Surf. Process. Landf.* 42, 1597–1600.

593 Kennedy, D.M.; Stephenson, W.J., and Naylor, L.A., 2014. *Rock coast geomorphology: A global
594 synthesis*, Kennedy, D.M.; Stephenson, W.J., and Naylor, L.A., (eds.). London: Geological Society,
595 292p.

596 Kuhn, D., and Prüfer, S., 2014. Coastal cliff monitoring and analysis of mass wasting processes with
597 the application of terrestrial laser scanning: A case study of Rügen, Germany. *Geomorphology*, 213,
598 153–165.

599 Lageat, Y.; Hénaff, A., and Costa, S., 2006. The retreat of the chalk cliffs of the Pays de Caux
600 (France): erosion processes and patterns. *Zeitschrift für Geomorphologie*, N. F. Suppl. 144, 183–197.

601 Lahousse, P., and Pierre, G., 2002. The retreat of chalk cliffs at Cape Blanc-Nez (France): Autopsy of
602 an erosion crisis. *Jour. Coastal Res.*, 19, 431–440.

603 Laignel, B., 1997. Les altérites à silex de l'ouest du Bassin de Paris: caractérisation lithologique,
604 genèse et utilisation potentielle comme granulats. Rouen, France: PhD Thesis.

605 Laignel, B., 2003. Caractérisation et dynamique érosive de systèmes géomorphologiques continentaux
606 sur substrat crayeux. Exemple de l'Ouest du Bassin de Paris dans le contexte nord-ouest européen.
607 HDR, Université de Rouen. 138p.

608 Lasseur, E., 2007. La Craie du Bassin de Paris (Cénomaniens-Campaniens, Crétacé supérieur).
609 Sédimentologie de faciès, stratigraphie séquentielle et géométrie 3D. Rennes, France: Université
610 Rennes 1, Thèse de doctorat.

611 Le Cossec, J., 2010. La déformation gravitaire des côtes à falaises sédimentaires : modélisation
612 numériques et expérimentales du secteur côtier Le Havre-Antifer (Haute-Normandie). Le Havre,
613 France: Université du Havre, Thèse de doctorat.

614 Letortu, P., 2013. Le recul des falaises crayeuses haut-normandes et les inondations par la mer en
615 Manche centrale et orientale : de la quantification de l'aléa à la caractérisation des risques induits.
616 Caen, France: Université de Caen, Thèse de doctorat.

617 Letortu, P. ; Costa, S. ; Bensaid, A.; Cador, J.-M., and Quénot, H., 2014. Vitesses et modalités de recul
618 des falaises crayeuses de Haute-Normandie (France): méthodologie et variabilité du recul.
619 *Géomorphologie, Relief, Processus and Environnement*, 20, 133–144.
620 <https://doi.org/10.4000/geomorphologie.10872>

621 Letortu, P.; Costa, S.; Cador, J.-M.; Coinaud, C., and Cantat, O., 2015a. Statistical and empirical
622 analyses of the triggers of coastal chalk cliff failure. *Earth Surf. Process. Landf.*, 40, 1371–1386.

623 Letortu, P.; Costa, S.; Maquaire, O.; Delacourt, C.; Augereau, E.; Davidson, R.; Suanez, S., and
624 Nabucet, J., 2015b. Retreat rates, modalities and agents responsible for erosion along the coastal chalk
625 cliffs of Upper Normandy: The contribution of terrestrial laser scanning. *Geomorphology*, 245, 3–14.

- 626 Lim, M., 2014. The rock coast of the British Isles: cliffs. *In*: Kennedy, D.M.; Stephenson, W.J., and
627 Naylor, L.A. (eds.), *Rock Coast Geomorphology: A Global Synthesis*, London, Geological Society,
628 *Book*, 40, pp. 19–38.
- 629 Lim, M.; Petley, D. N.; Rosser, N. J.; Allison, R. J.; Long, A. J., and Pybus, D., 2005. Combined
630 digital photogrammetry and time-of-flight laser scanning for monitoring cliff evolution. *The*
631 *Photogrammetric Record*, 20(110), 109-129.
- 632 Lim, M.; Rosser, N.J.; Allison, R.J., and Petley, D.N., 2010. Erosional processes in the hard rock
633 coastal cliffs at Staithes, North Yorkshire. *Geomorphology*, 114, 12–21.
- 634 Lissak, C., 2012. Les glissements de terrain des versants côtiers du pays d’Auge (Calvados) :
635 morphologie, fonctionnement et gestion du risque. Caen, France: Université de Caen, Thèse de
636 doctorat de Géographie.
- 637 Lissak, C.; Maquaire, O., and Malet, J.-P., 2009. Role of hydrological process in landslide occurrence:
638 Villerville-Cricqueboeuf landslides (Normandy coast, France). *In*: Malet, J.-P.; Remaître, A., and
639 Boogard, T.A., (eds.), *Proceedings of the International Conference on Landslide Processes: from*
640 *geomorphologic mapping to dynamic modelling*. Strasbourg, CERG Editions, pp.175-180.
- 641 Lissak, C.; Maquaire, O.; Malet, J.-P., and Davidson, R., 2014. Piezometric thresholds for triggering
642 landslides along the Normandy coast, France. *Géomorphologie*, 2, 145-158.
- 643 Lissak, C.; Puissant, A.; Maquaire, O., and Malet, J.-P., 2013. Analyse spatio-temporelle de
644 glissements de terrain littoraux par l’exploitation de données géospatiales multi-sources. *Revue*
645 *internationale de géomatique*, 2, 199-225.
- 646 Maquaire, O., 1990. Les mouvements de terrain de la côte du Calvados - Recherche et prévention.
647 *Document du BRGM*, No. 197.
- 648 Maquaire, O.; Afchain, P.; Launay, A.; Costa, S.; Lissak, C.; Fressard, M.; Letortu, P.; Davidson, R.
649 and Thiery, Y. 2013. Evolution à long terme des falaises des 'Vaches Noires' et occurrence des
650 glissements (Calvados, Basse-Normandie, France). *In*: *Recueil des actes des Journées 'Aléas*
651 *Gravitaire'*, Grenoble, 17-18 septembre.
- 652 Marques, F.M.S.F, 2006. Rates, patterns and timing of cliff retreat. A case study on the west of
653 Portugal. *Zeitschrift für Geomorphologie*, Supplementbande No 144, 231-257.
- 654 May, V.J., and Heeps, C., 1985. The nature and rates of change on chalk coastlines. *Zeitschrift für*
655 *Geomorphologie*, 57, 81–94.
- 656 Medjkane, M.; Maquaire, O.; Costa, S.; Roulland, Th.; Letortu, P.; Fauchard, C.; Antoine, R., and
657 Davidson, R., 2018. High resolution monitoring of complex coastal morphology changes: cross-
658 efficiency of SfM and TLS-based survey (Vaches-Noires cliffs, Normandy, France). *Landslides*, 15,
659 1097-1108.
- 660 Michoud, C.; Carrea, D.; Costa, S.; Derron, M-H.; Jaboyedoff, M.; Delacourt, C.; Maquaire, O.;
661 Letortu, P., and Davidson, R., 2014. Landslides Detection and Monitoring Capability of Boat-based
662 Mobile Laser Scanning along Dieppe Coastal Cliffs, Normandy. *Landslides journal*. DOI
663 10.1007/s10346-014-0542-5
- 664 Moore, L.J., 2000. Shoreline mapping techniques. *Journal of Coastal Research*, 16(1), 111-124.
- 665 Moore, L.J., and Griggs, G.B., 2002. Long-term cliff retreat and erosion hotspots along the central
666 shores of the Monterey Bay National Marine Sanctuary. *Marine Geology*, 181, 265-283.

667 Mortimore, R.N.; Lawrence, J.; Pope, D.; Duperret, A., and Genter, A., 2004. Coastal cliff geohazards
668 in weak rock: the UK Chalk cliffs of Sussex. *In: Mortimore, R.N., and Duperret, A. (eds.), Coastal*
669 *Chalk Cliff Instability*, London, Geological Society, *Engineering Geology* Special Publication, 20, pp.
670 3-31.

671 Moses, C.A., and Robinson, D., 2011. Chalk coast dynamics: Implications for understanding rock
672 coast evolution. *Earth-Science Reviews*, 109, 63–73.

673 Olsen, M.J.; Johnstone, E.; Kuester, F.; Driscoll, N., and Ashford, S.A., 2011. New automated Point-
674 Cloud Alignment for Ground-Based Lighth Detection and Ranging Data of Long Coastal Sections.
675 *Journal of Surveying Engineering*, 137(1), 14-25.

676 Paskoff, R., 1998. *Les littoraux : impact des aménagements sur leur évolution*. Paris: Masson, 184p.

677 Peruccacci, S.; Brunetti, M.T.; Gariano, S.L.; Melillo, M.; Rossi, M., and Guzzetti, F., 2017. Rainfall
678 Thresholds for Possible Landslide Occurrence in Italy. *Geomorphology*, 290, 39- 57.
679 <https://doi.org/10.1016/j.geomorph.2017.03.031>.

680 Pierre, G., and Lahousse, P., 2006. The role of groundwater in cliff instability: an example at Cape
681 Blanc-Nez (Pas-de-Calais, France). *Earth Surface Processes Landforms*, 31, 31–45.

682 Pomerol, B.; Bailey, H. W.; Monciardini, C., and Mortimore, R.N., 1987. Lithostratigraphy and
683 biostratigraphy of the Lewes and Seaford chalks : a link across the Anglo-Paris basin at the Turonian-
684 Senonian boundary. *Cretaceous Research*, 8, 289-304.

685 Prager, C.; Zangerl, C.; Patzelt, G., and Brandner, R., 2008. Age distribution of fossil landslides in the
686 Tyrol (Austria) and its surrounding areas. *Natural Hazards and Earth System Sciences*, 8, 377-407.

687 RIEGL Laser Measurement Systems, 2014. Datasheet VZ-400 (RIEGL Laser Measurement Systems
688 GmbH). Austria

689 Rosser, N.J.; Brain, M.J.; Petley, D.N.; Lim, M., and Norman, E.C., 2013. Coastline retreat via
690 progressive failure of rocky coastal cliffs. *Geology*, 41, 939-942.

691 Rosser, N.J.; Petley, D.N.; Lim, M.; Dunning, S.A., and Allison, R.J., 2005. Terrestrial laser scanning
692 for monitoring the process of hard rock coastal cliff erosion. *Quarterly Journal of Engineering*
693 *Geology and Hydrgeology*, 38, 363-375.

694 Roulland, Th.; Maquaire, O.; Costa, S.; Compain, V.; Davidson, R., and Medjkane, M. Accepted.
695 Dynamique des falaises des Vaches Noires : analyse diachronique historique et récente à l'aide de
696 documents multi-sources (Normandie, France). *Géomorphologie, Relief, Processus, Environnement*.

697 Senfaute, G.; Duperret, A., and Lawrence, J. A., 2009. Micro-seismic precursory cracks prior to rock-
698 fall on coastal chalk cliffs: a case study at Mesnil-Val, Normandie, NW France. *Natural Hazards and*
699 *Earth System Sciences*, 9, 1625-1641.

700 Sunamura, T., 1992. *Geomorphology of Rocky Coasts*. Chichester: Wiley.

701 Thenhaile, A.S., 1987. *The geomorphology of Rock Coasts*, *Oxford Research Studies in Geography*.
702 Oxford: Clarendon Press-Oxford, 384p.

703 Trenhaile, A.S., 2011. Cliffs and Rock Coasts. *In: Flemming, B.W. and Hansom, J.D. (eds.), Treatise*
704 *on Estuarine and Coastal Science*. Amsterdam: Elsevier, vol. 3, pp.171-192.

705 Trenhaile, A.S., 2000. Modeling the development of wave-cut shore platforms. *Marine Geology*, 166,
706 163-178.

707 Vioget, A., 2015. Analyse de l'évolution morpho-structurale des falaises littorales du Bessin, Basse-
708 Normandie, France. Lausanne, Suisse: Université de Lausanne, Institut des Sciences de la Terre,
709 Mémoire de master, 100p. et annexes.

710 Woodroffe, C.D., 2002. *Coasts: Form, process and evolution*. Cambridge: University of Cambridge
711 Press, 625p.

712 Young, A.P.; Guza, R.T.; Flick, R.E.; O'Reilly, W.C., and Gutierrez, R., 2009. Rain, waves, and short-
713 term evolution of composite seacliffs in southern California. *Marine Geology*, 267, 1–7.

714 Young, A.P., and Ashford, S.A., 2006. Application of airborne LIDAR for seacliff volumetric change
715 and beach sediment contributions. *Journal of Coastal Research*, 22, 307-318.

716 Zêzere, J.L. 2002. Landslide susceptibility assessment considering landslide typology. A case study in
717 the area north of Lisbon (Portugal). *Natural Hazards and Earth System Science*, 2 (1/2), 73–82.

718 Zêzere, J.L.; Vaz, T.; Pereira, S.; Oliveira, S.C.; Marques, R., and Garcia., R.A.C., 2015. Rainfall
719 Thresholds for Landslide Activity in Portugal: A State of the Art. *Environmental Earth Sciences*,
720 73(6), 2917- 2936. <https://doi.org/10.1007/s12665-014-3672-0>.
721

722 **Websites:**

723 SNO-DYNALIT, French national observatory for coastal dynamics from National Institute of science
724 of the Universe, 2018. <https://www.dynalit.fr/>

725 SNO-OMIV, Multidisciplinary Observatory of Versant Instabilities, 2018. <https://omiv.osug.fr/>

726 INEE “Zones Ateliers”, French National Institute on Ecology and Environment Studies, 2018.
727 <http://www.za-inee.org>
728

729

730

731